Dynamic Lamb-dip effects in gas lasers with inhomogeneously broadened saturable absorbers

C. R. Carvalho and L. Davidovich
Departamento de Física, Pontifícia Universidade Católica do Rio de Janeiro, Caixa Postal 38071, 22452 Rio de Janeiro, Rio de Janeiro, Brazil

(Received 2 January 1991; revised manuscript received 25 March 1991)

We show, through a simple model, that as one changes the detuning of a standing-wave single-mode gas laser containing an inhomogeneously broadened saturable absorber, a Lamb-dip generated stability window may appear in the instability region. The width of this window is of the order of the homogeneous linewidth of the absorber, and it is not affected by power broadening.

PACS number(s): 42.55.Lt, 42.65.Pc

I. INTRODUCTION

Passive Q switching (PQS) of a CO_2 laser containing an intracavity saturable absorber is a phenomenon well known from the early development of this infrared laser [1–7]. PQS occurs in a single-mode laser, as opposed to pulsing in mode-locked lasers. It represents thus a single-mode instability, the electric-field amplitude being modulated in time with a period determined by the relaxation parameters of the gain medium and of the absorber. The origin of this modulation is the "mode-splitting" effect discussed by Casperson and Yariv [8] within the context of inhomogeneously broadened lasers: for the same integer number of wavelengths in the cavity, multiple steady-state solutions for the frequency of oscillations may appear, due to the dispersive behavior of the intracavity medium which may manifest itself even in a resonant situation. This happens because the effective laser frequency depends on the field intensity through a nonlinear relation (the linear version of this relation yields the "frequency-pulling" formula). For lasers with saturable absorbers, it was shown by Mandel [9] that a similar effect may arise, since, again due to the nonlinear dependence of the oscillation frequency on the intensity, the absorptive cavity becomes dispersive for a suitable domain in parameter space.

A simple model describing a standing-wave laser with a saturable absorber was proposed by Powell and Wolga [2]. They adopted a two-level description of both the amplifier and the absorber, and predicted, through a rate-equation treatment, a bistable regime for the laser intensity, determining at the same time the conditions for PQS. Deeper analyses of this system have been carried out by several authors [3–7,9–11], leading to many interesting features, beyond the self-pulsing instability, which have been the subject of both experimental and theoretical investigations. The effect of extra nonresonant levels has been considered [5–7,11], and it has been shown that this system may exhibit Hopf bifurcations and chaotic behavior [5,11].

In most of these references, both the gain and the absorbing media have been modeled as being homogeneously broadened. In fact, even though this is frequently not true in the experiments performed so far, taking inhomogeneous broadening into account is usually a formidable theoretical task, involving cumbersome expressions and a large amount of computing time. One hopes then that inhomogeneous broadening would have a small effect on the final results. One expects this to be especially true if one is interested in time-dependent phenomena with a time scale much larger than the atomic collision time, since velocity redistribution collisions eventually should allow all the atoms in the Doppler profile to participate in the process (collisional "hole filling") [12].

This has not precluded, however, the observation of shallow Lamb dips in CO_2 lasers [13], or even of a central tuning peak (inverted Lamb dip) due to a low-pressure CO_2 absorber [2,14]. This inverted dip is due to the saturation of the group of absorbing molecules with zero speed, which interact resonantly with both counterpropagating beams. Therefore, the absorber gets less effective around resonance, within a region of frequencies limited by the power-broadened homogeneous linewidth of the absorber. Furthermore, typical inhomogeneous broadening effects in self-pulsing gas lasers have been put into evidence recently. Thus, Gioggia *et al.* [15] have demonstrated experimentally a Lamb-dip-like behavior of the pulsing frequency in a standing-wave single-mode He-Xe laser. A similar behavior was verified by Alcantara, Jr. and Rios Leite, in a CO_2 laser with an intracavity saturable absorber [16].

An experimental and theoretical investigation of passive Q switching in a CO_2 laser with a hot CO_2 internal absorbing cell was made by Brzhazovskii *et al.* [3]. Their modelization takes into account the inhomogeneous broadening of both the gain and the absorber media, and leads to numerical results for the single-mode instability threshold in agreement with the experimental data.

A detailed theoretical treatment of a gas laser with an inhomogeneously broadened saturable absorber was also presented by Salomaa and Stenholm [10], who discussed the generation of multimode instabilities in the regime where the atomic populations can be adiabatically eliminated (good-cavity limit). In this case, the mode coupling provided by the nonlinear absorber accounts for the energy transfer from a strongly oscillating mode to other cavity eigenmodes, located within the gain bandwidth, which may thus undergo self-sustained oscillations. The dispersive effect of the intracavity medium was neglected, and therefore no discussion was presented of the single-

mode instabilities mentioned above, which become the sole source of pulsing when the intermode spacing is sufficiently large. They may show up whenever the longitudinal relaxation constants for the amplifier and the absorber become of the same order or smaller than the field decay constant so that we are in a regime where the adiabatic elimination of the populations is not allowed (we may still proceed to the adiabatic elimination of the polarizations, however, since in CO_2 lasers transverse relaxation is usually much faster than the other processes).

In this paper we show that inhomogeneous broadening may affect the single-mode self-pulsing or otherwise unstable regime in a quite dramatic way. Under some conditions, one can get windows of stability, as the laser detuning is changed. These regions are generated by a Lamb-dip behavior of the complex eigenfrequency associated with the initial oscillations around the steady state, and their width is of the order of the homogeneous broadening of the absorber.

This result may be considered in fact to complement those of Ref. [15]. The complex eigenfrequency comes out from the linear stability analysis, its imaginary part being just the frequency of the initial oscillations around the steady state. At the same time, its real part controls the stability of the cw solution and, through the quantum regression theorem [17], yields in the stable case the linewidth of the spectrum of fluctuations. In Ref. [15], one looks at the dependence of the imaginary part of the complex frequency on the detuning. Here, we focus on the real part, which may change signs when the laser is detuned over the Lamb-dip region, thus affecting the stability of the cw solution.

At first sight, it would seem that these effects could be interpreted as a mere consequence of the Lamb-dip behavior of the intensity, due to the dependence of the complex eigenfrequency on the steady-state intensity. This is not so, however, since the width of the dips here observed is not affected by power broadening. In fact, the expression *Lamb dip* is used here in a generalized sense, taken to include not only the dip in the intensity, but also any analog manifestation, on any variable of the system, of the resonant interaction between the zero-velocity molecular group and the two counterpropagating beams in a standing-wave gas laser.

Our results are based on a simple two-level model for the amplifier and absorbing media. This is certainly an oversimplification, since it is known that the rotovibrational levels of both media play an important role in the time-dependent behavior of the system [5–7,11]. The two-level model fits, however, our objective of displaying the novel Lamb-dip effects in the simplest possible way, so as to make it easier to grasp the underlying physical phenomena.

II. A RATE-EQUATION MODEL

We assume that the transverse relaxation rates for the amplifier and the absorber are much larger than the rate of change of the other variables, as is usually the case in CO_2 lasers with hot CO_2 absorbers, so that the polarization can be adiabatically eliminated [17]. Even though we are considering a standing-wave laser, we neglect the spatial dependence of the population inversion densities, since in a gas laser the molecules actually experience an averaged intensity, because of their fast motion, as compared to the population decay time [17]. We get then a set of rate equations for the photon number density S and the inversion densities of the amplifier n (representing the number of molecules in the upper state minus the number of molecules in the lower state per unit volume) and the absorber $\bar{n}(v)$ (representing the number of molecules in the lower state minus the number of molecules in the upper state per unit of volume and velocity),

$$\dot{n}=-\gamma_{\parallel}(n-n_0)-\alpha(\omega)nS\ , \tag{1a}$$

$$\dot{\bar{n}}(v)=-\bar{\gamma}_{\parallel}[\bar{n}(v)-\bar{n}_0(v)]-\beta(\omega,v)\bar{n}(v)S\ , \tag{1b}$$

$$\dot{S}=-\gamma_C S+\alpha(\omega)nS-\int_{-\infty}^{+\infty}dv\,\beta(\omega,v)\bar{n}(v)S\ . \tag{1c}$$

Here $\alpha(\omega)$ is the atom-field interaction coefficient for the gain medium and for a field angular frequency ω (all our frequencies and decay constants are specified in rad/s), $\beta(\omega,v)$ is the corresponding quantity for the absorber, while $\gamma_{\parallel}$, $\bar{\gamma}_{\parallel}$, and γ_C are the relaxation rates for the amplifier, the absorber, and the field, respectively. Finally, n_0 and $\bar{n}_0(v)$ are the amplifier and absorber inversion densities in the absence of the laser field but in the presence of pumping.

The coefficient $\alpha(\omega)$ is given by

$$\alpha(\omega)=\frac{\mu^2\omega}{2\hbar\gamma_{\perp}\epsilon_0}\frac{\gamma_{\perp}^2}{\gamma_{\perp}^2+\Delta\omega^2}\ , \tag{2}$$

where μ is the magnitude of the transition dipole for the amplifier, $\gamma_{\perp}$ is the gain medium bandwidth (which is just the polarization relaxation rate), $\Delta\omega$ is the atom-field detuning, and ϵ_0 is the vacuum dielectric constant. On the other hand, $\beta(\omega,v)$ is given by

$$\beta(\omega,v)=\frac{\bar{\mu}^2\omega}{4\hbar\bar{\gamma}_{\perp}\epsilon_0}\left[\frac{\bar{\gamma}_{\perp}^2}{\bar{\gamma}_{\perp}^2+(\Delta\omega+kv)^2}+\frac{\bar{\gamma}_{\perp}^2}{\bar{\gamma}_{\perp}^2+(\Delta\omega-kv)^2}\right]\ , \tag{3}$$

where $k=\omega/c$, and $\bar{\mu}$ is the magnitude of the absorber transition dipole. This expression exhibits the Doppler broadening due to the molecular velocity distribution. The two Lorentzians correspond to the interaction of the group of molecules with velocity v with the two counterpropagating running modes which form the standing-wave field.

The gain medium is considered to be homogeneously broadened, since its pressure is usually much greater (one to three orders of magnitude) than that of the absorbing gas, so that the homogeneous linewidth ($\gamma_{\perp}$) gets larger than the Doppler one. On the other hand, we have for the absorber

$$\bar{n}_0(v)=\frac{\exp[-(v/\bar{v})^2]}{\bar{v}\sqrt{\pi}}\bar{n}_0 , \tag{4}$$

where $\bar{v}=(2KT/m)^{1/2}$ is the average speed of the gas molecule, m is its mass, T is the temperature, K is the Boltzmann constant, and $\bar{n}_0$ (without the v argument) is the total inversion density for the absorber.

Equations (1) are similar to those discussed by Powell and Wolga [2], with the only difference that Eq. (1c) incorporates the contribution of the entire absorber line profile, as considered in Refs. [3] and [10]. Our equations are in fact a particular case of the corresponding ones in Ref. [3], where the inhomogeneous broadening of the absorber was also taken into account. The specialization to an homogeneously broadened absorber allows us to make a more detailed analysis of the system than the one made in Ref. [3].

We find now the steady-state solutions of these equations, and show that they may display a bistable behavior.

III. BISTABLE BEHAVIOR

The steady state of the system is obtained by setting the time derivatives in Eqs.(1a)–(1c) equal to zero,

$$n_{st}=\frac{n_0\gamma_\parallel}{\gamma_\parallel+\alpha(\omega)S_{st}} , \tag{5a}$$

$$\bar{n}_{st}(v)=\frac{\bar{n}_0(v)\bar{\gamma}_\parallel}{\bar{\gamma}_\parallel+\beta(\omega,v)S_{st}} , \tag{5b}$$

$$\gamma_C S_{st}=\alpha(\omega)n_{st}S_{st}-S_{st}\int_{-\infty}^{+\infty}dv\,\beta(\omega,v)\bar{n}_{st}(v) . \tag{5c}$$

As in Ref. 1, there is a trivial solution $S_{st}=0$. Further solutions can be obtained from the equation

$$\gamma_C=\frac{\alpha(\omega)\gamma_\parallel n_0}{\gamma_\parallel+\alpha(\omega)S_{st}}-\int_{-\infty}^{+\infty}dv\frac{\beta(\omega,v)\bar{\gamma}_\parallel\bar{n}_0(v)}{\bar{\gamma}_\parallel+\beta(\omega,v)S_{st}} , \tag{5d}$$

which is derived from (5c) by canceling out the common factor S_{st}. The right-hand side of the above equation is just the effective gain $G_{eff}(S_{st})$ of the laser, so (5d) expresses the threshold condition for laser operation: gain equals losses. Plotting G_{eff} and γ_C as functions of the steady-state intensity allows a qualitative analysis of the system behavior (Fig. 1). The intersections of these two curves will provide the extra steady-state solutions, besides the trivial one. We see from (5d) that G_{eff} decreases monotonically for large S_{st}. However, for small values of S_{st}, G_{eff} may present an initial increase with S_{st}, leading to two extra steady-state solutions and a possible bistable behavior (see Fig. 1). Conditions for this to happen can be easily figured out by expanding G_{eff} in a power series of S_{st}. We get then

$$G_{eff}(S_{st})=\alpha(\omega)n_0-\int_{-\infty}^{+\infty}dv\,\bar{n}_0(v)\beta(\omega,v)+S_{st}\left[\int_{-\infty}^{+\infty}dv\frac{\beta(\omega,v)^2\bar{n}_0(v)}{\bar{\gamma}_\parallel}-\frac{\alpha(\omega)^2n_0}{\gamma_\parallel}\right]+\cdots .$$

We see from this expression and from Fig. 1(b) that, in order to have the extra solutions, the linear term in S_{st} must be positive.

Figure 1 may also be used to analyze the stability of the solutions. Thus, in Fig. 1(a) only $S_{st}\neq 0$ can be stable, since for $S_{st}=0$ the gain overcomes the cavity loss rate, so that any small fluctuation will make the intensity

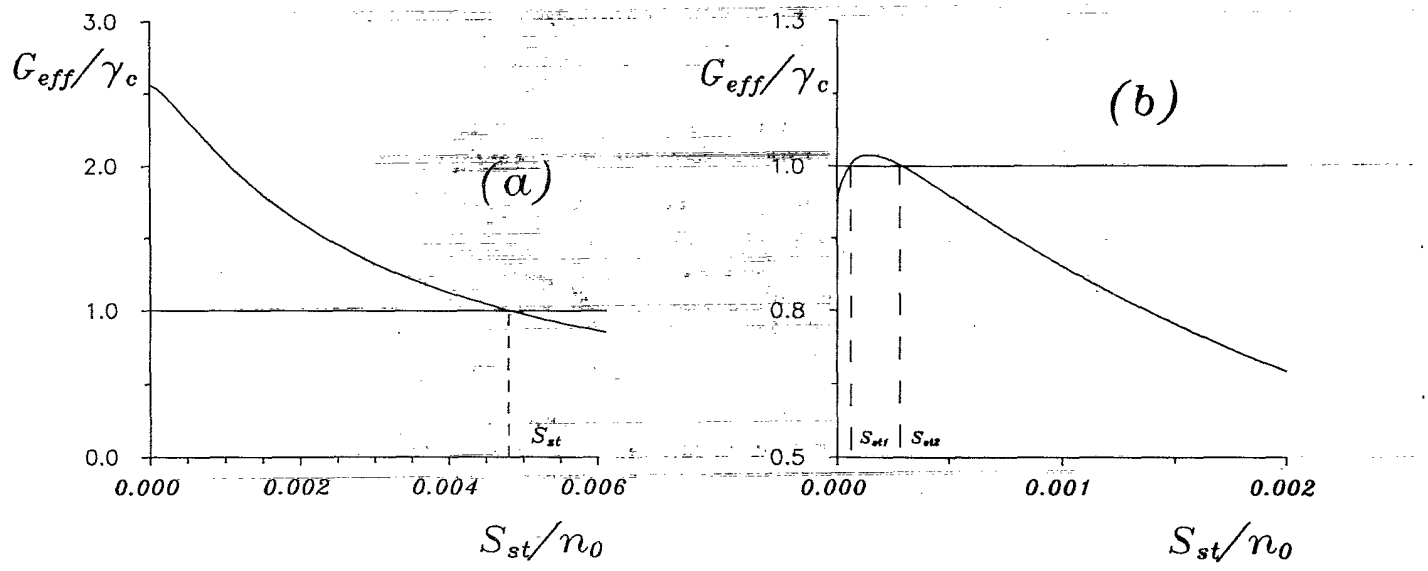

FIG. 1. Effective gain of the laser as a function of the steady-state photon density S_{st}. The horizontal line represents the losses. (a) The effective gain decreases monotonically and the system presents only one steady state. Here, $\mu=\bar{\mu}=0.87\times10^{-31}$ Cm, $\omega=2\pi\times3\times10^{13}$ rad/s, $n_0=3.0\times10^{19}\text{m}^{-3}$, $\gamma_\parallel=40\pi\times10^3$ rad/s, $r=\bar{\gamma}_\parallel/\gamma_\parallel=1.5$, $s=\bar{\gamma}_\perp/\gamma_\parallel=400$, $q=\gamma_C/\gamma_\parallel=125$, $z=\gamma_\perp/\gamma_\parallel=6900$, $p=\bar{n}_0/n_0=0.3$. (b) The effective gain has an initial increase due to the saturation of the absorption and the system presents bistable behavior. Same parameters as in (a), except for $r=0.5$ and $q=337.5$.

grow. Notice, however, that even though this simple graphical approach leads easily to the identification of unstable solutions, points here identified as stable may turn out to be unstable under a more detailed analysis, which takes into account the possibility of independent fluctuations of the inversion densities. This will be done in Sec. IV. In the present discussion, the fluctuations of the inversion densities are tied up to the field fluctuations through Eqs. (5a) and (5b), so that our analysis is in principle correct only in the regime in which the populations adiabatically follow the field ($\gamma_\parallel, \bar{\gamma}_\parallel \gg \gamma_C$). This is the regime considered, for instance, in Ref. [10], where a similar discussion was presented.

Proceeding with this simplified case, we see that for Fig. 1(b) two solutions are possible, besides the trivial one $S_{st}=0$. The figure suggests that the solution $S_{st}=0$ is now a stable one, since in this case the effective gain is less than the cavity loss rate. On the other hand, the solution S_{st_1} is unstable, since increasing the intensity by a small amount will cause the gain to become larger than the loss rate, so the intensity will keep increasing. By a similar argument, we can show that S_{st_2} is stable. We have thus in this case a bistable behavior.

In the next section we extend the above analysis in order to consider independent fluctuations of the inversion densities and the field. That is, we go beyond the adiabatic regime mentioned above (the polarization is still assumed to follow the other variables). We show then that some of the stable solutions found in this section may become unstable, giving rise to a self-pulsing behavior, still within the single-mode model.

IV. STABILITY ANALYSIS

We adopt the usual procedure [18] of linearizing Eqs. (1) around each steady state, getting in this way a set of equations for the population and field displacements. If the corresponding normal modes are damped, then the solution is stable; otherwise, it is unstable.

We set, therefore,

$$n(t)=n_{st}+\delta n(t) , \tag{6a}$$

$$\bar{n}(v,t)=\bar{n}_{st}(v)+\delta\bar{n}(v,t) , \tag{6b}$$

$$S(t)=S_{st}+\delta S(t) , \tag{6c}$$

so that, neglecting higher-order terms in δn, $\delta\bar{n}(v)$ and δS, we get

$$\delta\dot{n}=-\gamma_\parallel\delta n-\alpha S_{st}\delta n-\alpha n_{st}\delta S , \tag{7a}$$

$$\delta\dot{\bar{n}}=-\bar{\gamma}_\parallel\delta\bar{n}-\beta S_{st}\delta\bar{n}-\beta\bar{n}_{st}(v)\delta S , \tag{7b}$$

$$\delta\dot{S}=\left[\alpha\delta n-\int_{-\infty}^{+\infty}dv\,\beta\delta\bar{n}\right]S_{st} + \left[\alpha n_{st}-\int_{-\infty}^{+\infty}dv\,\beta\bar{n}_{st}(v)-\gamma_C\right]\delta S . \tag{7c}$$

We will be interested in the case $S_{st}\neq 0$. The last term on the right-hand side of (7c) is then equal to zero [cf. Eq. (5d)].

The normal modes of the above set of equations correspond to solutions of the form

$$\begin{bmatrix}\delta n(t)\\ \delta\bar{n}(v,t)\\ \delta S(t)\end{bmatrix}=\begin{bmatrix}\delta n_0\\ \delta\bar{n}_0(v)\\ \delta S_0\end{bmatrix}\exp(\lambda t) . \tag{8}$$

It is important to observe that (7) and (8) actually stand for an infinite set of equations, corresponding to the range of velocities from $-\infty$ to $+\infty$. Replacing (8) into (7), we obtain, after a little amount of algebra, the characteristic equation for λ,

$$\lambda=-\frac{\alpha(\omega)^2 n_{st}S_{st}}{\alpha(\omega)S_{st}+\gamma_\parallel+\lambda} + S_{st}\int_{-\infty}^{+\infty}dv\frac{\beta(\omega,v)^2\bar{n}_{st}(v)}{\beta(\omega,v)S_{st}+\bar{\gamma}_\parallel+\lambda} . \tag{9}$$

The steady state will be stable if all the roots of this equation have negative real parts. Then, the imaginary parts will yield the frequencies of the relaxation oscillations towards equilibrium. On the other hand, if at least one of the roots has a positive real part, the steady state will be unstable. The imaginary part of this root will then correspond to the frequency of the initial pulsation of the field, as it departs from the unstable steady-state value. In this case, the actual behavior of the field does not necessarily correspond to self-pulsing, and cannot be found by a linear stability analysis.

We search now for roots of Eq. (9) with a positive real part, which are the ones which yield the unstable behavior. The computing time involved in evaluating the roots of (9) is reduced by finding bounds to the region of the complex plane where the roots are located. We notice first that, since the coefficients of this equation are real, then if λ is a root with a nonvanishing imaginary part, its complex conjugate λ^* is also a root. So we can restrict our search to roots with a positive imaginary part.

By setting $\lambda=x+iy$, we get, for the imaginary part of (9),

$$1=\frac{\alpha(\omega)^2 n_{st}S_{st}}{[\alpha(\omega)S_{st}+\gamma_\parallel+x]^2+y^2} - S_{st}\int_{-\infty}^{+\infty}dv\frac{\beta(\omega,v)^2\bar{n}_{st}(v)}{[\beta(\omega,v)S_{st}+\bar{\gamma}_\parallel+x]^2+y^2} . \tag{10}$$

This equation shows that the roots of (9) are in a finite region of the complex plane, since as $\lambda\to\infty$ the right-hand side of (10) tends to zero while the left-hand side is always equal to one, so leading to a contradiction. One also gets, from (10), that

$$\frac{\alpha^2 n_{st}S_{st}}{(\alpha S_{st}+\gamma_\parallel+x)^2+y^2}>1 . \tag{11}$$

By setting $x=0$ in (11), we obtain an upper limit for the imaginary part of the roots, that is,

$$y_{max}=[\alpha^2 n_{st}S_{st}-(\alpha S_{st}+\gamma_\parallel)^2]^{1/2} . \tag{12}$$

Now setting $y=0$ in (11), we obtain for the real part

$$\alpha^2 n_{st}S_{st}>(\alpha S_{st}+\gamma_\parallel+x)^2 ,$$

which yields

$$(\alpha^2 n_{st} S_{st})^{1/2} > \alpha S_{st} + \gamma_{\parallel} + x \geq -(\alpha^2 n_{st} S_{st})^{1/2} .$$

The last inequality does not give us any further information, since we are interested only in $x > 0$. So for the real part we are restricted to the interval

$$x_{max} = (\alpha^2 n_{st} S_{st})^{1/2} - \alpha S_{st} - \gamma_{\parallel} > x \geq 0 . \quad (13)$$

Equations (12) and (13) establish bounds for the region where one can find the roots of (9) with $y > 0$. Within this region, we adopt now the following procedure. We divide the region in small rectangles and test for the central point of each piece if the function

$$f(\lambda) = \lambda + \frac{\alpha(\omega)^2 n_{st} S_{st}}{\alpha(\omega) S_{st} + \gamma_{\parallel} + \lambda} - S_{st} \int_{-\infty}^{+\infty} dv \frac{\beta(\omega, v)^2 \bar{n}_{st}(v)}{\beta(\omega, v) S_{st} + \bar{\gamma}_{\parallel} + \lambda} \quad (14)$$

is smaller than a critical value $\tilde{f}$. When this condition is satisfied, we consider this point as initial trial in the numerical routine ZANLYT of the IMSL [19], which yields then the roots of (14). Different partitions and critical values must be tried in order to check the procedure and make sure that no root is missed. We scan the region starting from x_{max}, since we are interested in the root with greatest real part. We repeat this procedure for each value of the detuning, being thus able to plot the real value of that root as a function of the detuning.

We discuss in the following section the results of this numerical analysis.

V. NUMERICAL RESULTS

In a typical experimental setup, the parameters that can be controlled in order to study the dependence on the detuning of the dynamics of the system are the pressure and the temperature of the gain and absorbing media, the pumping discharge current of the gain medium, and the reflectivity of the cavity mirrors. In the theoretical description we deal instead with the inversion and polarization decay rates of both media, the Doppler bandwidth of the absorber (which depends on $\bar{v}$), the zero-field inversion densities, and the cavity decay rate. We have chosen for these parameters values which stay close to typical experimental conditions, for the case of a hot CO_2 absorbing cell [16].

We take $\mu = \bar{\mu} = 0.87 \times 10^{-31}$ Cm, $\omega = 6\pi \times 10^{19}$ rad/s. For the gain medium we consider the inversion and polarization relaxation rates of the order of $40\pi \times 10^4$ rad/s and $2\pi \times 138 \times 10^6$ rad/s, respectively, corresponding to a pressure of about 20 Torr (note that angular frequencies are used throughout). For the absorber the polarization relaxation rate is taken to be of the order of $16\pi \times 10^6$ rad/s, corresponding to a pressure of the order of 1 Torr. The ratio between the inversion and polarization decay rates of both media are assumed to have the same order of magnitude, since the dependence of the relaxation rates on the pressure is approximately linear (they are not precisely the same, however, since the gain medium usually involves a mixture of CO_2, N_2, and He, while the absorber is composed only of CO_2). However, the effective lifetime of a molecule of the absorber, moving across the laser beam, is taken as a combination of the inversion lifetime $T_{\parallel}$ with the average transit time across the beam T_{tr}, that is,

$$\bar{\gamma}_{\parallel} = \frac{1}{T_{eff}} = \frac{1}{T_{\parallel}} + \frac{1}{T_{tr}} . \quad (15)$$

The first term on the right-hand side of (15) is the inversion decay rate which should be of the order of $2\pi \times 10^3$ rad/s. The second term has a maximum value of the order of $2\pi \times 5 \times 10^4$ rad/s for molecules with velocities orthogonal to the beam. So the mean value of the effective lifetime is compatible with a decay rate of the order of $2\pi \times 3 \times 10^4$ rad/s, adopted by us in the numerical calculations. The temperature of the absorber is typically of 600 K, which corresponds to $\bar{v}$ of the order of 500 m/s. Considering the pressure of the gases, the pumping discharge current and the dimensions of the cells containing the gases, the zero-field inversion of the gain medium is approximately 10^{18}–10^{19} molecules/m^3 and for the absorber we have the third or fourth part of this. For a cavity length of $L = 1.2$ m with an output mirror transmissibility of the order of 2%, the field decay rate is $\gamma_C = 2\pi \times cT/2L = 2\pi \times 2.5 \times 10^6$ rad/s. The corresponding mode separation $c/2L$ is of the order of $2\pi \times 125 \times 10^6$ rad/s. Although still smaller than the gain bandwidth ($2\pi \times 138 \times 10^6$ rad/s) — two cavity modes fit into the gain profile — this is usually sufficient to inhibit multimode operation, since most frequently for only one of the modes will gain overcome the losses (actually, for a homogeneously broadening gain medium, as assumed here, gain clamping should occur, so only one of the modes would oscillate). For these typical experimental values, we are in fact in the limit of applicability of the adiabatic elimination of the polarization, since $\bar{\gamma}_{\perp}/\gamma_C \approx 3.2$.

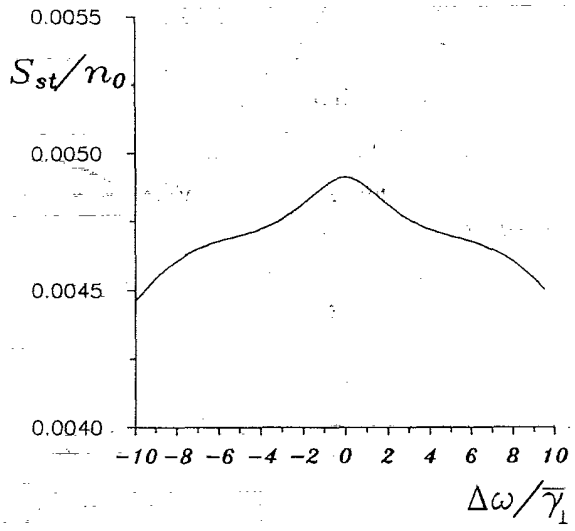

FIG. 2. Normalized steady-state photon density S_{st}/n_0 as a function of the normalized detuning $\Delta\omega/\bar{\gamma}_{\perp}$. Same parameters as in Fig. 1(a).

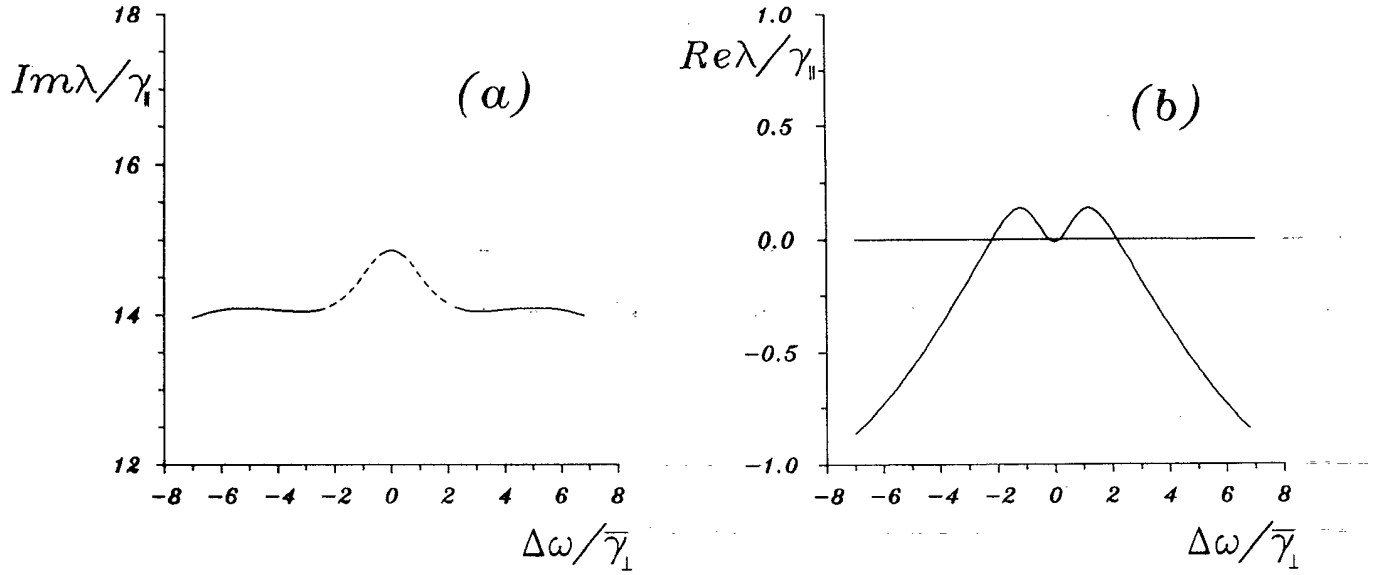

FIG. 3. (a) Imaginary part of λ as a function of the detuning (solid line corresponds to the stable regime, dashed line to the unstable one); (b) real part of λ as a function of the detuning. Same conditions as for Fig. 2.

The numerical solution of Eq. (9) was found in terms of the set of parameters n_0, $\gamma_\parallel$, $p=\overline{n}_0/n_0$, $q=\gamma_C/\gamma_\parallel$, $r=\overline{\gamma}_\parallel/\gamma_\parallel$, $s=\overline{\gamma}_\perp/\gamma_\parallel$, and $z=\gamma_\perp/\gamma_\parallel$. We discuss here the results corresponding to a particular set, associated with a situation in which the power-broadened absorber homogeneous linewidth is comparable with the inhomogeneous broadening. For this particular set of parameters, the system is not bistable, its steady-state behavior being the one depicted in Fig. 1(a).

The order of magnitude of the inhomogeneous broadening is given by the product of $\overline{v}$ with the wave number k, so that $\gamma_{\rm in}=k\overline{v}$. On the other hand, the power-broadened homogeneous linewidth $\overline{\gamma}_{\perp p}$ of the absorber may be estimated from the expression for the population inversion of the non absorbing atoms with zero velocity,

$$\overline{n}_{\rm st}(0)=\frac{\overline{n}_0(0)\overline{\gamma}_\parallel}{\overline{\gamma}_\parallel+\beta(0)S_{\rm st}}=\frac{\overline{n}_0(0)(\overline{\gamma}_\perp^2+\Delta\omega^2)}{\Delta\omega^2+\overline{\gamma}_\perp^2(1+S_{\rm st}/I_S)},$$

so that $\overline{\gamma}_{\perp p}=\overline{\gamma}_\perp\sqrt{1+S_{\rm st}/I_S}$, where $I_S=\hbar\epsilon_0\overline{\gamma}_\parallel\overline{\gamma}_\perp/\mu^2\omega$ is the saturation intensity.

For $n_0=3.0\times10^{19}$ m^{-3}, $\gamma_\parallel=40\pi\times10^3$ rad/s, $r=1.5$, $q=125$, $s=400$, $z=6900$, $p=0.3$, and $\overline{v}=500$ m/s, we get $\overline{\gamma}_{\perp p}/\overline{\gamma}_\perp\approx5.0$, and $\gamma_{\rm in}/\overline{\gamma}_{\perp p}\approx1.25$. The photon density $S_{\rm st}$ in this case is plotted in Fig. 2. We notice that, superimposed to a hole in the photon-density curve, due to the presence of the inhomogeneously broadened absorbing molecules, there is an antidip, with power-broadened width $\overline{\gamma}_{\perp p}$.

In Fig. 3(a) we plot the oscillation frequency $\Omega=\mathrm{Im}(\lambda_>)$ as a function of the detuning, where $\lambda_>$ is the root of Eq. (9) with the greatest real part. It displays clearly an antidip [Fig. 3(a)], *which is, however, not power broadened.* Therefore, the antidip in the oscillation frequency cannot be attributed to the intensity dependence of the eigenvalue $\lambda_>$. It can be traced back to the stronger dependence on $\beta(\omega,v)$ of λ, due to the extra $\beta(\omega,v)$ factor in the integrand on the right-hand side of Eq. (9), with respect to the integrand in Eq. (5d), which yields the steady-state values of the intensity.

In Fig. 3(b) we display the behavior of the real part of $\lambda_>$ as a function of the detuning. It presents a Lamb dip, also with a width of the order of $\overline{\gamma}_\perp$. But the most important feature is that, as exemplified in Fig. 3(b),the dip may cause a sign change of Re ($\lambda_>$), and therefore an abrupt modification in the behavior of the laser.

The different regions determined by this behavior of Re($\lambda_>$) are displayed in Fig. 3(a). When Re($\lambda_>$)<0, Ω

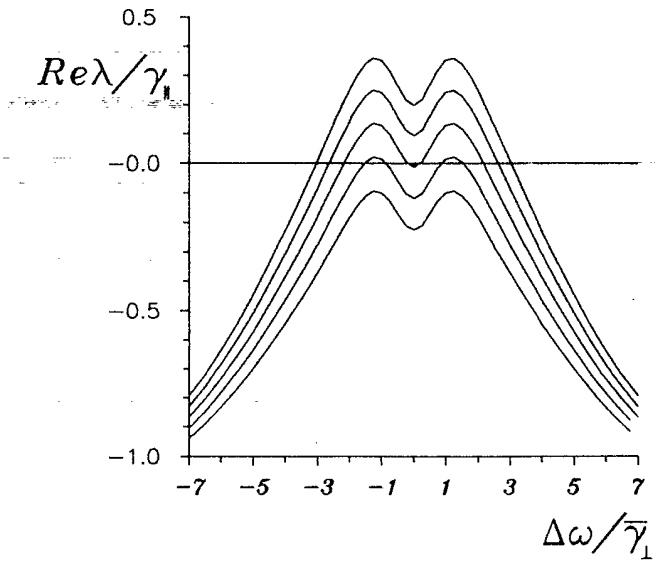

FIG. 4. Dependence of Reλ on the parameter $r=\overline{\gamma}_\parallel/\gamma_\parallel$, the other parameters remaining fixed. From top to bottom $r=1.7, 1.6, 1.5, 1.4, 1.3$.

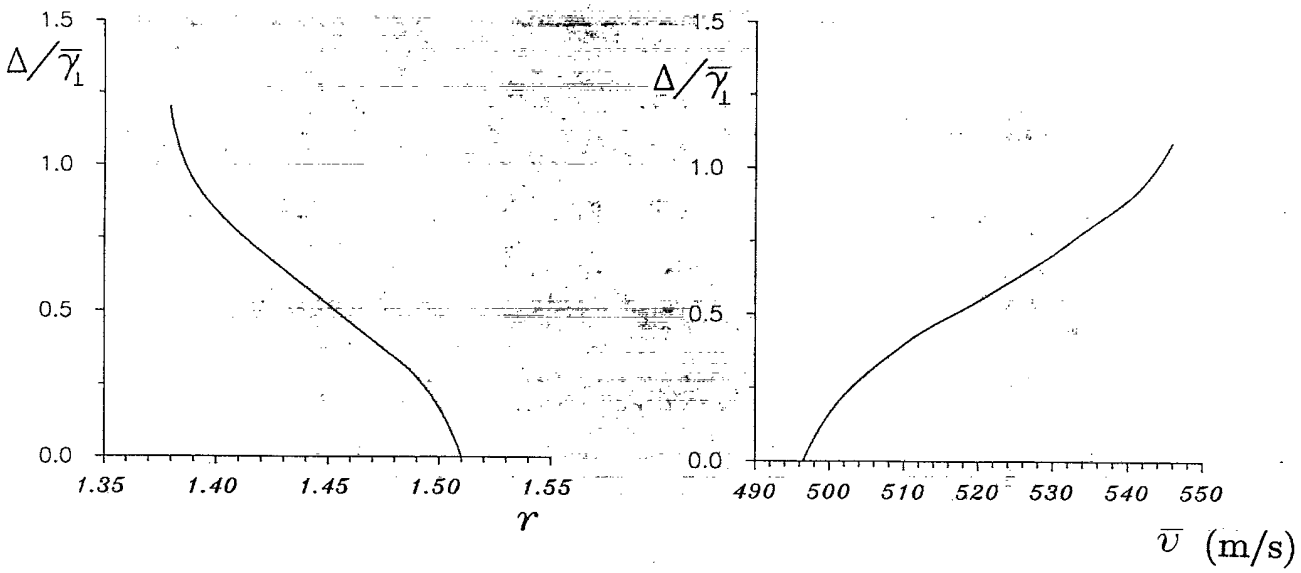

FIG. 5. Half-width of the cw window as a function of $r=\overline{\gamma}_\parallel/\gamma_\parallel$.

FIG. 7. Half-width of the cw window as a function of $\overline{v}$.

represents the frequency of the relaxation oscillations towards equilibrium, since the laser is then in cw operation (solid line). On the other hand, when $\mathrm{Re}(\lambda_>)>0$, Ω stands for the frequency of the initial oscillations away from the steady-state value (dashed line). If the corresponding instability is a PQS, then this Ω should be approximately equal to the pulsation frequency if the magnitude of the pulsations is not too large.

Changing the parameter r, while at the same time keeping fixed the other parameters, amounts to displacing vertically the curve for $\mathrm{Re}(\lambda_>)$, as shown in Fig. 4. This will affect the width of the cw region. Changing $\overline{v}$ or p will produce the same effect. In Fig. 5, we display the half-width of the cw window as a function of r. As r increases, the width decreases from a value of the order of $\overline{\gamma}_\perp$ to zero. On the other hand, these parameters affect very little, in this region, the pulsation frequency Ω. In Figs. 6 and 7 we display the half-width of the cw window as a function of p and $\overline{v}$, respectively.

One should remark that a Lamb-dip structure of the instability region may also show up in a multimode gas laser, where it is possible to suppress oscillation of a weak mode, due to the self-saturation of a strong mode. This was discussed in detail in Ref. [10]. It is important to notice, however, that the mechanism of suppression of oscillations is quite different in our case, since we are dealing with a single-mode case, the instabilities being generated by nonlinear dispersive effects ("mode splitting"). In particular, as opposed to the multimode laser, the width of the stability region is not affected by power broadening in our case.

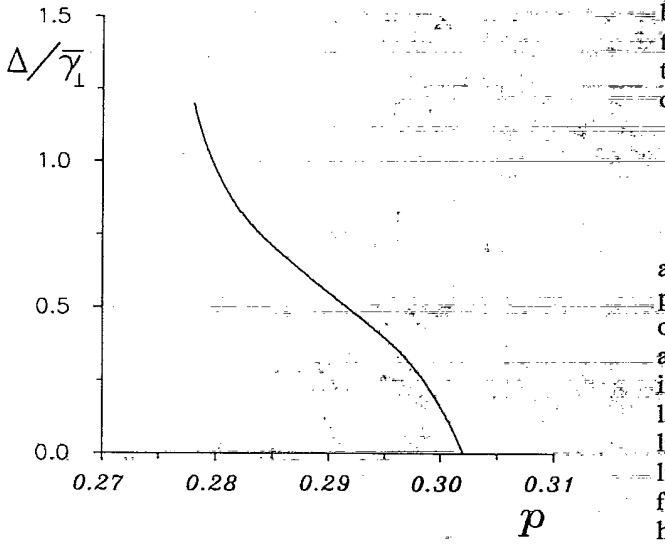

FIG. 6. Half-width of the cw window as a function of $p=\overline{n}_0/n_0$.

VI. CONCLUSION

We have shown that the inhomogeneous broadening of a saturable absorber placed inside a gas laser cavity may produce interesting effects in the unstable single-mode operation. Not only may the pulsing frequency exhibit an antidip as the laser tuning is changed, as demonstrated in Ref. [15], but the instability may cease altogether, the laser becoming stable as a consequence of a Lamb-dip like behavior of the complex eigenfrequencies of the linear stability analysis. The stability window thus formed has a maximum width which is of the order of the homogeneous linewidth of the absorber, and, contrary to what happens to the intensity, it is not affected by power broadening. It offers therefore a new possibility for a more precise Lamb-dip stabilization of the laser.

We have adopted the strategy of demonstrating these effects within the framework of a very simplified model. It would be certainly interesting to check the effect of other levels, and especially of the rotovibrational relaxation, on the above results. Also, in order to study the time-dependent behavior of the system in the instability region a nonlinear numerical calculation must be made. Work along these lines is in progress, and will be reported elsewhere.

ACKNOWLEDGMENTS

The authors are grateful to J. R. Rios Leite and P. A. Alcantara, Jr. for introducing them to the problem of lasers with inhomogeneously broadened saturable absorbers, for informing about the values of the experimental parameters, and for many helpful discussions. This work has been partially supported by CNPq, CAPES, FAPERJ, and FINEP.

[1] O. R. Wood and S. E. Schwarz, Appl. Phys. Lett. **11**, 88 (1967); P. L. Hanst, J. A. Morreal, and W. J. Hanson, *ibid.* **12**, 58 (1968); J. T. Yardley, *ibid.* **12**, 120 (1968); N. V. Karlov, G. P. Kuz'min, Yu. N. Petrov, and A. M. Prokhorov, Pis'ma Zh. Eksp. Teor. Fiz. **7**, 174 (1968) [JETP Lett. **7**, 134 (1968)]; T. Y. Chang, C. H. Wang, and P. K. Cheo, Appl. Phys. Lett. **15**, 157 (1969).

[2] H. T. Powell and G. J. Wolga, IEEE J. Quantum Electron. **QE-7**, 213 (1971).

[3] Yu. V. Brzhazovskii, L. S. Vasilenko, S. G. Rautian, G. S. Popova, and V. P. Chebotaev, Zh. Eksp. Teor. Fiz. **61**, 500 (1971) [Sov. Phys.—JETP **34**, 265 (1972)].

[4] L.Lugiato, P. Mandel, S. T. Dembinski, and A. Kossakowski, Phys. Rev. A **18**, 238 (1978); J. C. Antoranz, J. Gea, and M. G. Velarde, Phys. Rev. Lett. **47**, 1895 (1981); J. C. Antoranz, L. L. Bonilla, J. Gea, and M. G. Velarde, *ibid.* **49**, 35 (1982).

[5] M. Tachikawa, K. Tanii, and T. Shimizu, J. Opt. Soc. Am. B **4**, 387 (1987); **5**, 1077 (1988); K. Tanii, M. Tachikawa, M. Kajita, and T. Shimizu, *ibid.* **5**, 24 (1988); M. Tachikawa, F-L. Hong, K. Tanii and T. Shimizu, Phys. Rev. Lett. **60**, 2266 (1988).

[6] E. Arimondo, F. Casagrande, L. Lugiato, and P. Glorieux, Appl. Phys. B **30**, 57 (1983).

[7] M. L. Asquini and F. Casagrande, Nuovo Cimento D **2**, 917 (1983).

[8] L. W. Casperson and A. Yariv, IEEE J. Quantum Electron. **QE-8**, 69 (1972).

[9] P. Mandel, Phys. Lett. **A83**, 207 (1981).

[10] R. Salomaa and S. Stenholm, Phys. Rev. A **8**, 2695 (1973), **8**, 2711 (1973).

[11] D. Hennequin, F. de Tomasi, B. Zambon, and E. Arimondo, Phys. Rev. A **37**, 2243 (1988); F. De Tomasi, D. Hennequin, B. Zambon, and E. Arimondo, J. Opt. Soc. Am. B **6**, 45 (1989); B. Zambon, F. De Tomasi, D. Henequin, and E. Arimondo, Phys. Rev. A **40**, 3782 (1989).

[12] T. Kan and G. J. Wolga, IEEE J. Quantum Electron. **QE-7**, 141 (1971).

[13] C. Bordé and L. Henry, IEEE J. Quantum Electron. **QE-4**, 874 (1968); T. Kan, H. T. Powell, and G. J. Wolga, *ibid.* **QE-5**, 297 (1969).

[14] P. H. Lee and M. Skolnik, Appl. Phys. Lett. **10**, 303 (1967); V. N. Lisitsyn and V. P. Chebotaev, Zh. Eksp. Teor. Fiz. **54**, 419 (1968) [Sov. Phys.—JETP **27**, 227 (1968)].

[15] R. S. Gioggia, N. B. Abraham, W. Lange, M. F. H. Tarroja, and J. C. Wesson, J. Opt. Soc. Am. B **5**, 992 (1988).

[16] C. K. Rhodes and A. Szöke, in *Laser Handbook,* edited by F. T. Arecchi and E. O. Schulz-Dubois (North-Holland, Amsterdam, 1972), Vol. 1, p. 298; A. E. Siegman, *Lasers* (University Science, New York, 1986); also J. W. R. Tabosa and J. R. Rios Leite, Opt. Lett. **10**, 544 (1985); **11**, 566 (1986); P. A. Alcantara, Jr., M. S. thesis, Universidade Federal de Pernambuco, Brazil, 1988.

[17] M. Sargent III, M. O. Scully, and W. E. Lamb, Jr., *Laser Physics* (Addison-Wesley, Redwood, 1987).

[18] H. Haken, *Synergetics—An Introduction* (Springer-Verlag, Berlin, 1983); L. M. Narducci and N. B. Abraham, *Laser Physics and Laser Instabilities* (World Scientific, Singapore, 1988); N. B. Abraham, P. Mandel, and L. M. Narducci, in *Progress in Optics,* edited by E. Wolf (North-Holland, Amsterdam, 1988), Vol. XXV, p. 1; P. W. Milonni, M-L. Shi, and J. R. Ackerhalt, *Chaos in Laser-Matter Interactions* (World Scientific, Singapore, 1987).

[19] W. H. Press, B. P. Flannery, S. A. Teukolsky, and W. T. Vetterling, *Numerical Recipes* (Cambridge University Press, Cambridge, 1986).